AMM12
The Second TSME International Conference on Mechanical Engineering
19-21 October, 2011, Krabi

The Influence of K-dominance Zone on Brittle Fracture

Suvanit Chitsiriphanit

Department of Mechanical and Aerospace Engineering, Faculty of Engineering,
King Mongkut's University of Technology North Bangkok, Bangkok, Thailand 10800
Corresponding Author: suvanitc@kmutnb.ac.th, Tel: 02 9132500, Fax: 02 5869541

Abstract

This paper presents a review of works in relation to the studies of K-dominance zone on brittle materials. It is commonly believed that stress intensity factor alone can characterize brittle fracture behavior. Researchers show that apparent fracture toughness under different specimen configurations and loading conditions is not constant due to the degree of K-dominance zone. It is found that the non-singular stress term combining with the stress singularity can be used to compute critical stress intensity factor effectively. The constant stress term acting ahead of the crack tip is represented by the positive or negative slope of the normalized opening stress. It is shown that the results obtained from the two-parameter model are in good agreement with the experiments.

Keywords*:* K-dominance zone, Non-singular stress term and Stress intensity factor

1. Introduction

An analysis of the linear elastic crack tip stress field assumes that the stress states are controlled by a single parameter, namely the stress intensity factor. Significant quantitative changes could occur when the first non-singular terms of the crack tip series expansion are included. This second parameter corresponds to the uniform stress term at crack tip. In particular, brittle fracture is a major mode of failure in components and structures containing cracks. Several researchers [1-5] have found that critical stress intensity factor or plane strain fracture toughness can be dependent on specimen geometries. Larsson and Carlsson [1] analyzed different specimen geometries and found that the effect of boundary around the crack tip can play an important role in determining the size of a crack tip plastic zone. William's asymptotic crack tip solution [6] was used to explain the yield zone sizes. The solution was modified by including the influence of the non-singular, constant second term in a series expansion. Further work extended by Leevers and Radon [2] showed the effect of specimen dimensions on stress biaxiality ratio, which is a function of constant stress terms, with different crack length sizes but same specimen configurations. Later, Kardomateas, et al. [3] showed the effect of short crack length sizes on stress biaxiality ratio, as described by Leevers and Radon [2]. Similar concepts conducted by Chao, et al. [4], they examined the variation of the apparent fracture toughness with constraint in mode I brittle

fracture. The results showed that the apparent fracture toughness increases with increasing first non-singular term. Liu, et al. [5] tested compact tension and single edge notch specimens made from PMMA to show the effect of constraint and different cracked specimen on brittle fracture of solids under mode I loading conditions. It was found that the apparent fracture toughness of the material depends on the constraining effect and geometry. Second and third terms of Williams's series solution were included to interpret these results.

This paper presents the experimental results, theoretical aspects and finite element analyses of the various specimen geometries and loading conditions. Middle crack specimens were conducted by Sun, et al. [7] in order to study the constraining effect and similar works were extended by Chitsiriphanit, et al. [8] using single edge notch specimens. The results showed that the critical stress intensity factor is not always constant due to the degree of K-dominance zone. Dominancy of stress singularity increases as K-dominance zone size increases. Hence, the two-parameter model, which is the non-singular stress term combining with the stress intensity factor, was proposed to predict apparent fracture toughness very accurately.

2. Experimental Methods

All the experiments were carried out on PMMA (trade-name: Plexiglas), which were tested under four point bending test and tensile test. The purpose of the tests is to determine fracture load. The test specimens consist of three groups as follows: six sizes of middle crack tension specimen (M-T) with various gage length ratio (h/a), six sizes of single edge tension specimen (SE-T) with various gage length ratio (h/a), and four sizes of single edge four point bending specimen (SE-FPB) with various crack length ratio (a/W).

2.1 Specimen Preparation

Various configurations of specimens were cut by water-jet as shown in Fig. 1. The thickness of Plexiglas panel was 4.76 and 5.77 mm for the test specimens. To make a sharp pre-crack of the specimen, a notch was carefully extended 2 mm by an incision with a razor blade. Fig. 2 shows sharp pre-crack on the surface and crack front inside material.

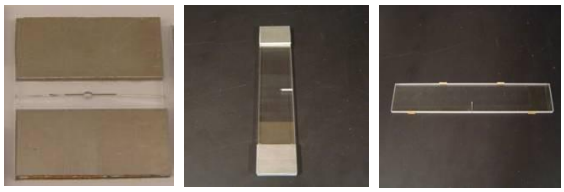

(M-T) (SE-T) (SE-FPB)

Fig. 1 M-T, SE-T and SE-FPB Specimens

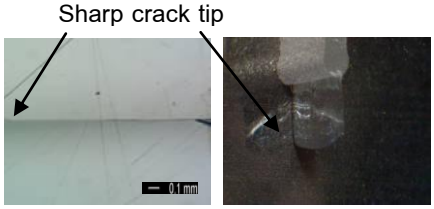

Fig. 2 Sharp Pre-Crack Created by Razor Blade

A middle crack PMMA specimen [7] for tensile test is shown in Fig. 3 below. The six sizes of different gage length ratio (h/a = 0.25, 0.50, 1, 2, 4 and 10) were considered to vary the constraining effect of the boundary on the crack and the value of the crack length ratio (a/W = 0.17) was kept constant. The thickness of the specimen was taken as 4.76 mm. Sharp pre-crack was created in all the specimens as described before. For the tensile test, aluminum

end tabs were used and attached onto the specimens by 3-M adhesive (DP-420).

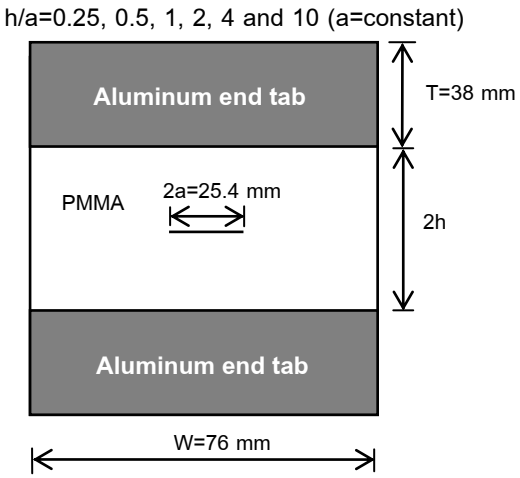

Fig. 3 Middle Crack Specimen for Tensile Test

For single edge notch tension [8], the detailed dimensions are shown in Fig. 4. To cover wide range of constraint level around the crack tip, the six sizes of different gage length ratio (h/a = 0.07, 0.13, 1, 2, 4 and 6) were considered and the value of the crack length ratio (a/W = 0.375) was kept constant. Thickness of the specimen was 5.77 mm. Aluminum tabs were attached using the adhesive DP-420.

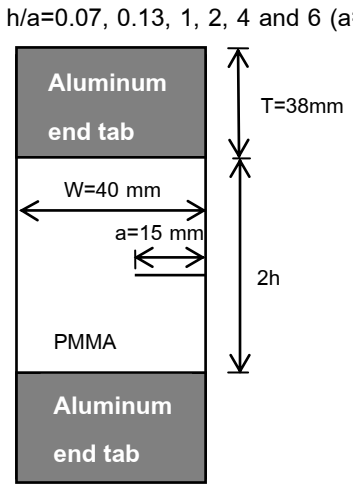

Fig. 4 SE-Notch Specimen for Tensile Test

Fig. 5 illustrates a typical specimen configuration of a single edge notch specimen for four point bending test [8]. To explore the influence of the crack length ratio (a/W), four values of the crack length ratio were considered: a/W = 0.375, 0.50, 0.625 and 0.75. Thickness of the specimen was 5.77 mm.

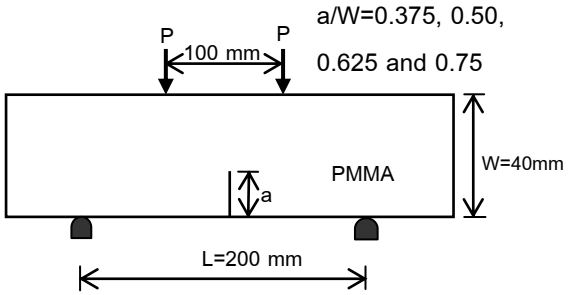

Fig. 5 SE-Notch Specimen for Four Point Bending Test

All the specimen geometries tested in this work were in plane strain condition.

2.2 Experimental Results

All the experiments were conducted at room temperature and performed on a servo controlled INSTRON testing machine. An MTS inductive extensometer, with ±1.0 mm nominal displacement and automatic calibration, was used to measure the load displacement point. The load was controlled and measured with a 22 Kips INSTRON load cell. All the tests were performed under displacement control at a rate of 0.001 mm/sec. As described in previous section, there are three groups of specimens for experiments in this study. During the tests, it was found that all the tensile and bending fractures occurred at maximum load without necking. Maximum loads were recorded in all the experiments. The test results for M-T, SE-T and SE-FPB are shown in Figs. 6-8 respectively.

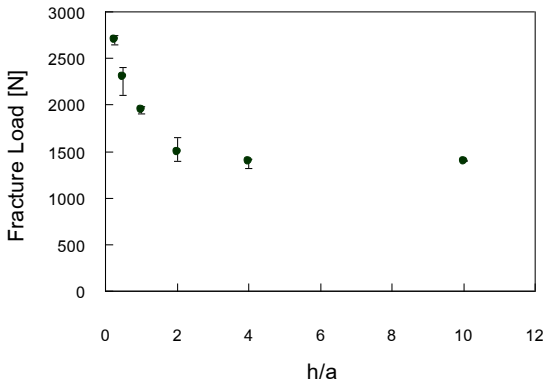

Fig. 6 Experimental Results of M-T

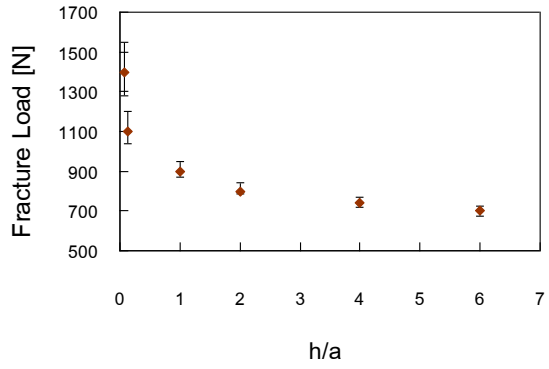

Fig. 7 Experimental Results of SE-T

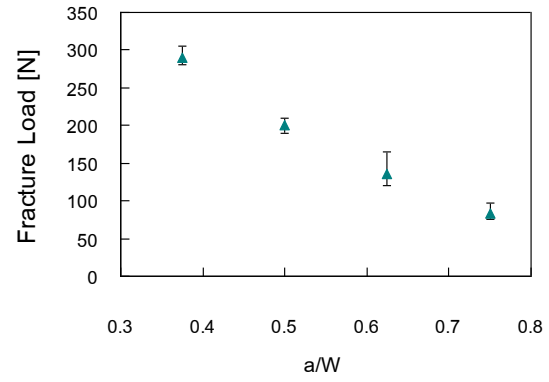

Fig. 8 Experimental Results of SE-FPB

From the test results, it is evident that for M-T and SE-T specimens with tensile test, the failure load of the specimens becomes higher as gage length decreases. It is interesting to note that as gage length (h/a) increases, the failure load approaches constant value. Contrary to SE-FPB specimens, the average fracture load of the specimens decreases as crack length ratio (a/W) increases. The maximum displacement at failure was applied to finite element model to capture critical strain energy release rate. The details will be described in the following section.

3. Apparent Fracture Toughness

To determine the apparent fracture toughness for all specimens, two dimensional linear elastic finite element analysis was performed for all cases using the commercial finite element code ABAQUS [10].

3.1 FEM Model Description

Considering the symmetry of the specimens, quarter symmetry models were used for M-T specimens and half symmetry models were used for SE-T and SE-FPB specimens as illustrated in Figs. 9 - 11 respectively.

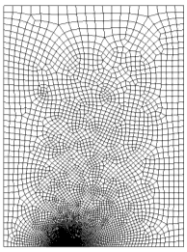

Fig. 9 Finite Element Model
(Quarter symmetry model) for M-T Model

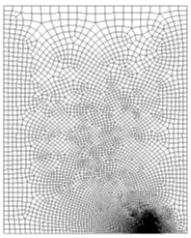

Fig. 10 Finite Element Model
(Half symmetry model) for SE-T Model

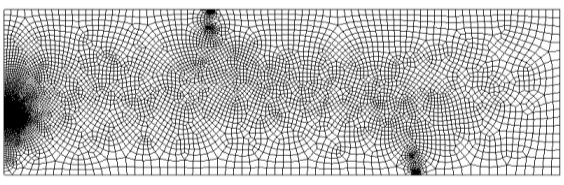

Fig. 11 Finite Element Model

(Half symmetry model) for SE-FPB Model

The structures were discretized into continuum elements featuring the 4-noded plane strain elements (CPE4). A very fine mesh was used in the highly stressed region of the components. The very small uniform mesh ($\Delta a/a$ less than 0.0001) around the crack tip was utilized to capture strain energy release rate. The values of elastic modulus $(E = 2.8\ GPa)$ and Poisson's ratio $(\nu = 0.3)$ are typical properties of PMMA.

3.2 FEM Results

In order to investigate the secondary fracture parameters, the normalized opening stress field can be obtained from numerical simulation by multiplying σ_{yy} with $\sqrt{2\pi x}$ and divided by stress intensity factor (K_I).

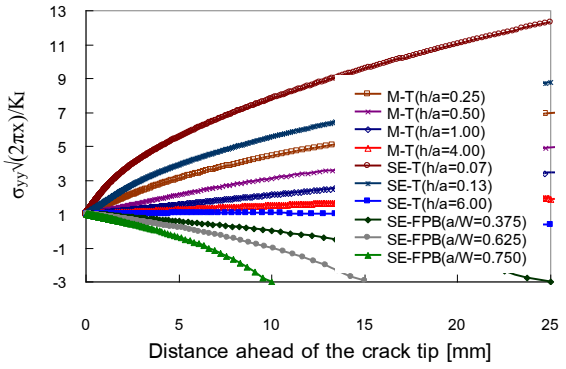

Fig. 12 Normalized Stress Distribution [25 mm] ahead of the Crack Tip

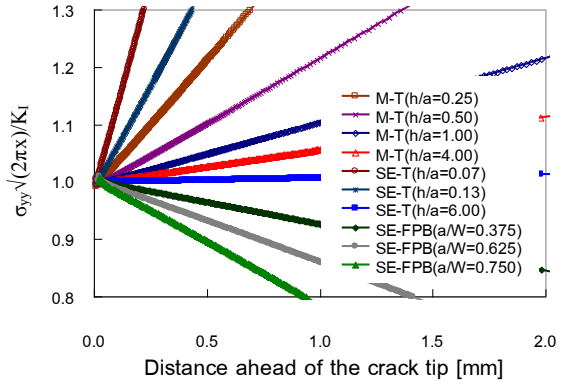

Fig. 13 Normalized Stress Distribution [2 mm] ahead of the Crack Tip

Figs. 12 - 13 present the plot of the following 10 specimens: M-T specimens with (h/a = 0.25, 0.50, 1 and 4), SE-T specimens with (h/a = 0.07, 0.13 and 6) and SE-FPB specimens with (a/W = 0.375, 0.625 and 0.75) to cover the wide range of slope. The increasing and decreasing slopes from the selected 10 specimens indicate that the stress singularity cannot fully describe the whole stress field ahead of the crack tip. In other words, the non-singular part of stress field becomes more important.

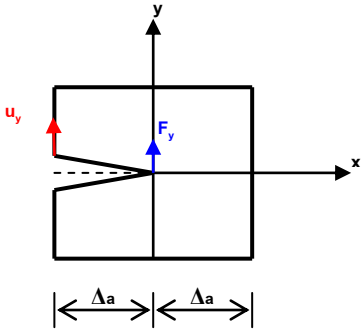

Fig. 14 Schematic of Modified Crack Closure Method for CPE4 Element

To obtain apparent fracture toughness of material, Modified Crack Closure Method (MCC) proposed by Rybicki and Kanninen [9], was used to calculate stress intensity factor. Fig. 14 shows the schematic view of Modified Crack Closure Method. The mesh near the crack tip must be very small and uniform.

$$G_I = \frac{F_y u_y}{\Delta a} \quad \text{(Symmetry Model) (1)}$$

$$G_I = \frac{K_I^2 (1-\nu^2)}{E} \quad \text{(Plane Strain) (2)}$$

where u_y is the vertical displacement and F_y is the vertical force. The strain energy release rate

(G_I) can be computed from Eq. (1) and then use G-K relation as given in Eq. (2) to convert (G_I) into stress intensity factor (K_I).

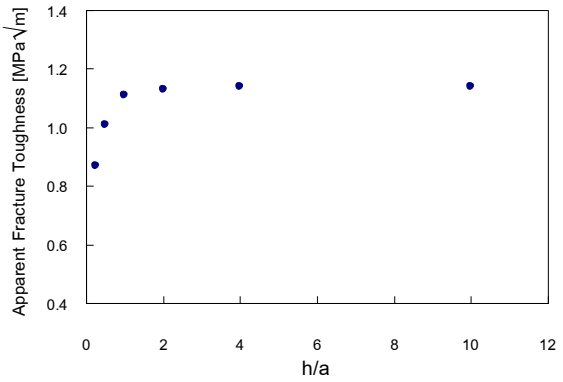

Fig. 15 Apparent Fracture Toughness (M-T) Determined by Modified Crack Closure Method

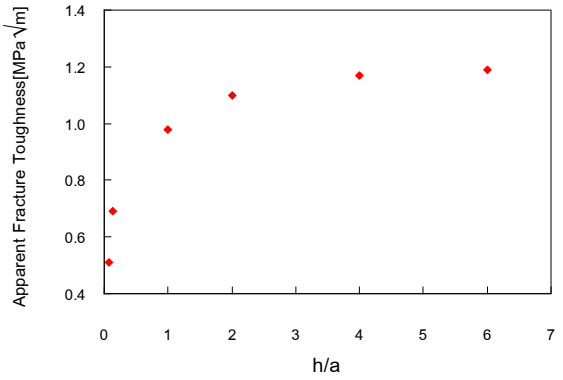

Fig. 16 Apparent Fracture Toughness (SE-T) Determined by Modified Crack Closure Method

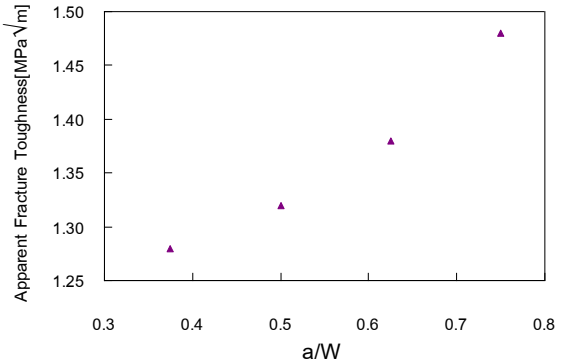

Fig. 17 Apparent Fracture Toughness (SE-FPB) Determined by Modified Crack Closure Method

It can be noted from Figs. 15 - 17 that apparent fracture toughness keep decreasing as gage length ratio (h/a) reduces in case of SE-T and M-T specimens. For SE-FPB specimens, apparent fracture toughness is higher as crack length ratio (a/W) increases.

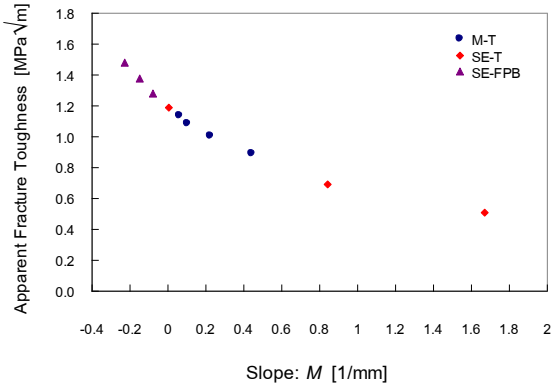

Fig. 18 Apparent Fracture Toughness Determined by Modified Crack Closure Method

It is interesting to note from the plot of the selected 10 specimens in Fig. 18 that all SE-FPB specimens have negative slope as all positive slopes appear within the region of all tensile specimens. To give an explanation, dominancy of stress singularity will be discussed in the following section and also two-parameter model will be proposed to predict fracture load.

4. K-dominance Zone Analysis

Within the framework of linear elastic fracture mechanics, one-parameter prediction (K_c) is used to characterize fracture toughness in brittle material if the singular stress field well represents the total stress field (σ_{yy}) ahead of the crack tip. Williams' asymptotic series solution [6] is employed to characterize the stress field near the crack tip in a linear elastic homogeneous and isotropic material. The opening stresses field can be written as

$$\sigma_{yy} = \frac{K_I}{\sqrt{2\pi x}} + C_0\sqrt{x} + \cdots \qquad (3)$$

The stress field in Eq. (3) ahead of the crack tip consists of stress singularity and non-singular parts. Stress intensity factor will be valid to predict fracture load when slope approaches zero as mentioned in the previous section. To analyze the K-dominance zone size, the non-singular stress term is needed. The degree of singularity dominance can be expressed as

$$\Lambda = \frac{K_I / \sqrt{2\pi x}}{K_I / \sqrt{2\pi x} + \left|\sigma_{yy}^{Non-Singular}\right|} \qquad (4)$$

where,

$$\sigma_{yy}^{Non-Singular} = \sigma_{yy} - \sigma_{yy}^{Singular} \qquad (5)$$

In this expression, the degree of K-dominance zone (Λ) as given in Eq. (4) can be explained as the ratio of singular stress and total stress field ahead of the crack tip. The distance from the crack tip of K-dominance zone size is determined within the region $\Lambda \geq 95\%$.

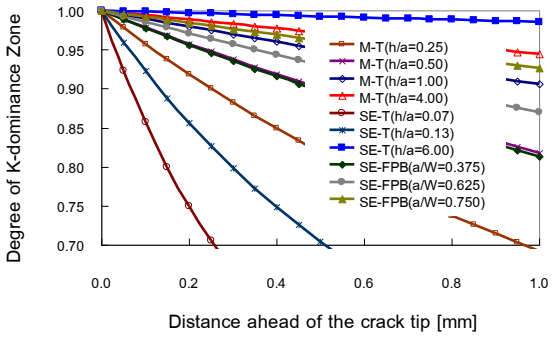

Fig. 19 Degree of K-dominance Zone along the Crack Line

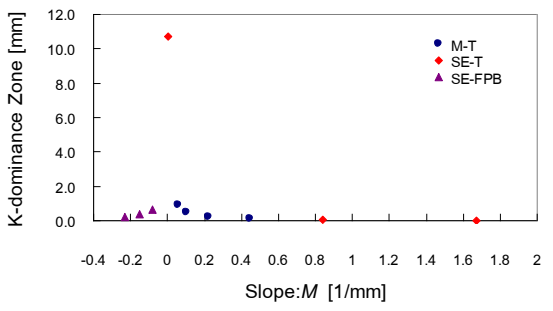

Fig. 20 K-dominance Zone Size (95%) VS. Slope: *M* [1/mm]

From Figs. 19 - 20, the degree of stress singularity for the selected ten test specimens shows that the K-dominance zone size is large when slope (*M*) approaches zero for the case of SE-T specimen with h/a = 6. Other than this region, the K-dominance zone size diminishes and the non-singular term will play an important role, which means that one-parameter prediction (K_c) is not suitable to predict failure load.

5. Two-Parameter Model

It is apparent from Fig. 20 that K-dominance zone sizes vary with the slope. In case of small K-dominance zone sizes, stress singularity alone cannot characterize brittle fracture. Therefore, non-singular stress term is needed to predict fracture load. To obtain this term, William's series expansion is rewritten as

$$\sigma_{yy}\sqrt{2\pi x} = K_I + C_0\sqrt{2\pi}x + \cdots \qquad (6)$$

As shown in Fig. 13, the values of normalized opening stress within distance [2 mm] ahead of the crack tip can be defined as linear part. The first two terms of William's series expansion can be represented as linear function.

$$\sigma_{yy}\sqrt{2\pi x}/K_I = 1 + \left(C_0\sqrt{2\pi}/K_I\right)x \qquad (7)$$

$$K_c^{\infty} = \sigma_{yy}\sqrt{2\pi x_0} = K_c\left(1 + Mx_0\right) \qquad (8)$$

$$K_c = K_c^{\infty} / \left(1 + x_0 M\right) \qquad (9)$$

The slope of SE-T specimen with h/a = 6 (K_c^{∞} = 1.20 $MPa\sqrt{m}$) is used as reference. *M* is slope [1/mm] measured from zero slope and x_0 = 0.77 mm is a constant critical length, which is determined from all ten experimental results. According to Eq. (9), the apparent fracture

toughness (K_c) can be computed using this proposed two-parameter model.

5.1 Comparison of Results

As described earlier, the variation of apparent fracture toughness is due to diminishing of K-dominance zone size. Using two-parameter model as proposed in previous section, the accurate results can be obtained as shown in the following plots, which illustrate the comparison of fracture load computed from two-parameter model and the results based on K_c-constant.

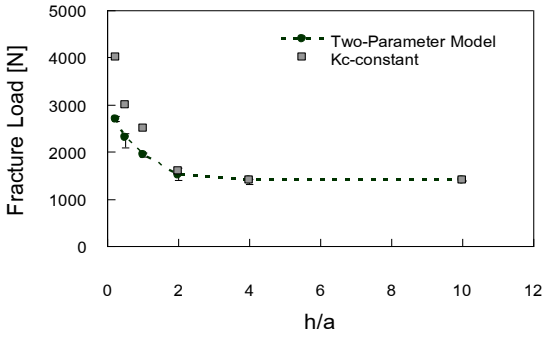

Fig. 21 Failure Load by the Two-Parameter Model for M-T Specimen

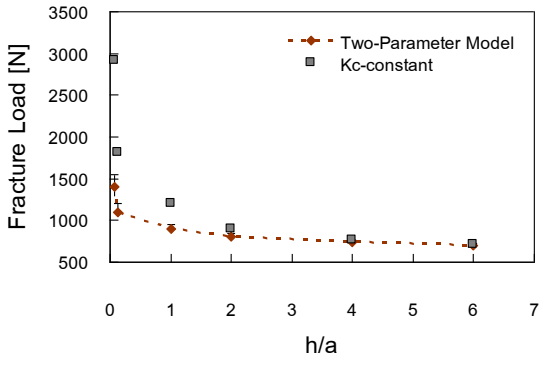

Fig. 22 Failure Load by the Two-Parameter Model for SE-T Specimen

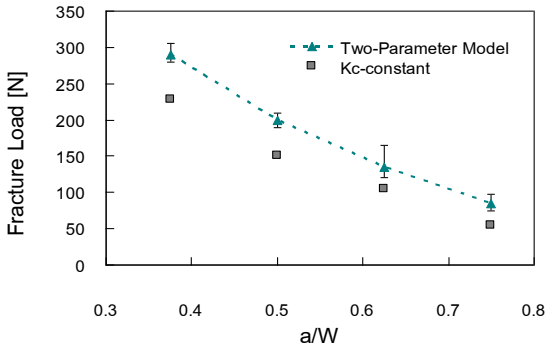

Fig. 23 Failure Load by the Two-Parameter Model for SE-FPB Specimen

Clearly, the results can be categorized into two groups as follows: Figs. 21 - 22 show that fracture loads under tensile test determined from the concept of K_c-constant are higher than the experimental results. As gage length (h/a) increases, fracture load based on K_c-constant will get close to the test results due to the larger K-dominance zone sizes. On the contrary, fracture load for SE-FPB tests computed from one-parameter (K_c-constant) will be less than the results from actual tests, which have negative slope as shown in Fig. 23.

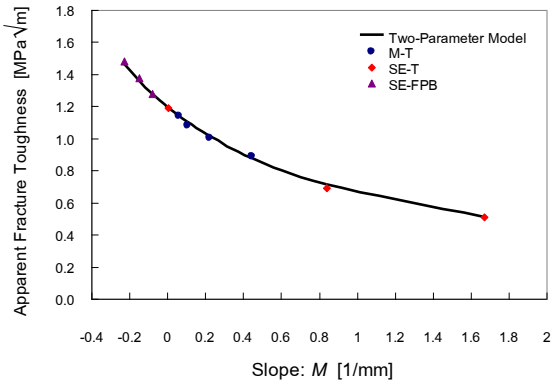

Fig. 24 Apparent Fracture Toughness VS. Slope: *M* [1/mm]

It can be seen in Fig. 24 that the apparent fracture toughness will be less than the proposed reference value (K_c^{∞}) in case of

positive slope and it will be higher for specimen configurations with negative slope. Using Eq. (9), apparent fracture toughness for brittle materials can be obtained by the slope corresponding to the specimen geometries and loading conditions.

6. Conclusions

In this work, mode I fracture tests were performed for three groups under different specimen configurations: middle crack tension, single edge tension and single edge four point bending. The results showed that apparent fracture toughness of brittle material is not constant and dependent on geometry of specimens and various types of loading conditions. The plot of normalized opening stress clearly showed that the apparent fracture toughness of M-T and SE-T specimens keeps decreasing as gage length ratio (h/a) reduces and their slopes become more positive. On the other hand, all the SE-FPB specimens have negative slope and apparent fracture toughness tends to increase as crack length ratio (a/W) increases.

An analysis of K-dominance zone size exhibited that the stress singularity is more suitable to characterize fracture toughness of brittle material as the slope approaches zero. In other word, the K-dominance zone size is large. Hence, the two-parameter model, which includes the slope of the nonsingular stress and the stress intensity factor was proposed and employed to calculate apparent fracture toughness very accurately.

7. Acknowledgement

Thankful for the support by the National Science and Technology Development Agency, Thailand.

8. References

[1] Larsson, S.G. and Carlsson, A.J. (1973). Influence of non-singular stress terms and specimen geometry on small-scale yielding at crack tips in elastic-plastic materials, *Journal of Mechanics and Physics of Solids*, vol. 21, 1973, pp. 263-277.

[2] Leevers, P.S. and Radon, J.C. (1982). Inherent stress biaxiality in various fracture specimen geometries, *International Journal of Fracture,* vol. 19, 1982, pp. 311-325.

[3] Kardomateas, G.A., Carlson, R.L., Soediono, A.H. and Schrage, D.P. (1993). Near tip stress and strain fields for short elastic cracks, *International Journal of Fracture,* vol. 62, 1993, pp. 219-232.

[4] Chao, Y.J., Liu, S. and Broviak, B.J. (2001). Brittle fracture: variation of fracture toughness with constraint and crack curving under mode I conditions, *Experimental Mechanics*, vol. 41(3), 2001, pp. 232-241.

[5] Liu, S. and Chao, Y.J. (2003). Variation of fracture toughness with constraint, *International Journal of Fracture,* vol. 124, 2003, pp. 113-117.

[6] Williams, M.L. (1957). On the stress distribution at the base of a stationary crack, *Journal of Applied Mechanics*, vol. 24, 1957, pp. 109-114.

[7] Sun, C.T. and Qian, H. (2009). Brittle fracture beyond stress intensity factor, *Journal of Mechanics of materials and structures*, vol. 4, 2009, pp. 743-753.

[8] Chitsiriphanit, S. (2010). On determination of apparent fracture toughness and fracture process zone, Ph.D. Dissertation, Purdue University, West Lafayette, Indiana.

[9] Rybicki, E.F. and Kanninan, M.F. (1977). A finite element calculation of stress intensity factors by a modified crack closure integral, *Engineering Fracture Mechanics,* vol. 9, 1977, pp. 931-938.

[10] Simulia Inc. (2009). *ABAQUS 6.9 Manual*, Providence, Rhode Island.